Eur. Phys. J. B **59**, 35–40 (2007)
DOI: 10.1140/epjb/e2007-00269-1

THE EUROPEAN PHYSICAL JOURNAL B

Spin hall accumulation in ballistic nanojunctions

S. Bellucci[1,a] and P. Onorato[1,2,3]

[1] INFN, Laboratori Nazionali di Frascati, P.O. Box 13, 00044 Frascati, Italy
[2] Department of Physics "A. Volta", University of Pavia, via Bassi 6, 27100 Pavia, Italy
[3] Dip. Ingegneria dell'Informazione, Seconda Università di Napoli, 81031 Aversa (CE), Italy

Received 4 May 2007 / Received in final form 12 July 2007
Published online 5 October 2007 – © EDP Sciences, Società Italiana di Fisica, Springer-Verlag 2007

Abstract. We propose a new scheme of spin filtering employing ballistic nanojunctions patterned in a two dimensional electron gas (2DEG). Our proposal is essentially based on the spin-orbit (SO) interaction generated by a lateral confining potential (β-SO coupling).
We demonstrate that the flow of a longitudinal unpolarized current through a ballistic T and X junction with this spin-orbit coupling will induce a spin accumulation which has opposite signs for the two lateral probes and is, therefore, the principal observable signature of the spin Hall effect in these devices.

PACS. 72.25.-b Spin polarized transport – 72.20.My Galvanomagnetic and other magnetotransport effects – 73.50.Jt Galvanomagnetic and other magnetotransport effects (including thermomagnetic effects)

1 Introduction

In recent years the increasing interest in spin-based information processing has fomented the field of semiconductor spintronics [1,2]. Several fundamental quantum phenomena which involve electron spin, have been investigated in order to generate and measure pure spin currents, i.e. not accompanied by any net charge current. Among these studies many are focused on the role of Spin Orbit (SO) couplings in condensed matter systems.

In the field of the spintronics a lot of attention was devoted to the Spin Hall Effect (SHE). The Hall effect is one of the most famous phenomena in condensed matter physics [3]: when electric current flows along a conductor subjected to a perpendicular magnetic field, the Lorenz force deflects the charge carriers creating a transverse Hall voltage between the lateral edges of the sample.

In analogy to the conventional Hall effect, an external electric field can be expected to induce a pure transverse spin current in the absence of applied magnetic fields. In fact the opposite spins can be separated and then accumulated on the lateral edges (2 and 4 in Fig. 1) when they are transported by a pure spin Hall current flowing in the transverse direction in response to an unpolarized charge current in the longitudinal direction (leads 1 and 3 in Fig. 1). Thus in order to give rise to the SHE the SO coupling has a central role. The SO Hamiltonian due to

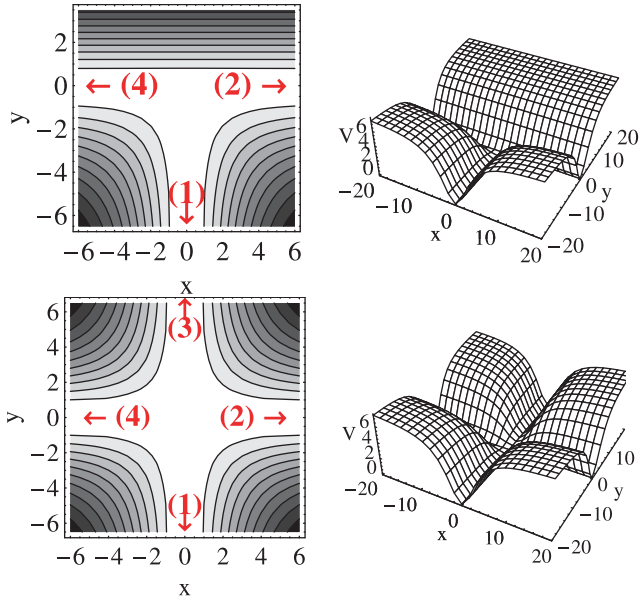

Fig. 1. Contour and 3D Plots of the potentials $V_c(x, y)$ which model a nanojunction. (Top) The typical 3-probe T junction (Bottom) the cross junction in the X geometry. The junctions in analogy with the devices proposed in reference [13] can be assumed as crossing junctions between two Q1D wires of width W which ranges from ∼25 nm up to 100 nm.

[a] e-mail: stefano.bellucci@lnf.infn.it

an electric field, $\mathbf{E}(\mathbf{r})$, is given by [4]

$$\hat{H}_{SO} = -\frac{\lambda_0^2}{\hbar}\, m_0 e \mathbf{E}(\mathbf{r}) \left[\hat{\sigma} \times \hat{\mathbf{p}}\right]. \tag{1}$$

Here m_0 denotes the electron mass in vacuum, $\hat{\sigma}$ are the Pauli matrices, $\hat{\mathbf{p}}$ is the canonical momentum operator $\mathbf{r}$ is a 3D position vector and $\lambda_0^2 = \hbar^2/(2m_0c)^2$. In semiconductors heterostructures, at whose interface the *two dimensional electron gas* (2DEG) is entrapped, m_0 and λ_0 are substituted by their effective values m^* and λ.

In this paper we consider low dimensional electron systems formed by quasi-one-dimensional (Q1D) devices patterned in 2DEGs. In such systems there can be different types of SO interaction [5] as: (i) the so-called Dresselhaus term which originates from the inversion asymmetry of the zinc-blende structure [6], (ii) the Rashba (α-coupling) term due to the quantum-well potential [7] that confines electrons to a 2D layer and (iii) the confining (β-coupling) term arising from the in-plane electric potential that is applied to squeeze the 2DEG into a Q1D channel [7,8].

Early theoretical studies predicted the SHE as an *extrinsic* effect due to impurities in the presence of SO coupling [9]. In this effect SO-dependent scattering of impurities will deflect spin-↑ (spin-↓) electrons predominantly to the right (left). More recently, it has been pointed out that there may exist a different SHE purely *intrinsic*. A pure transverse spin Hall current should be observed that is several orders of magnitude greater than in the case of the extrinsic effect, arising due to intrinsic mechanisms related to the spin-split band structure in SO coupled bulk [10,11] or mesoscopic [12] semiconductor systems.

Here we want discuss the presence of SHE in nanojunctions formed by crossing Q1D devices. The presence of SHE can be argued by the presence of a spin current or a spin accumulation as in reference [13] where the authors demonstrated that the flow of a longitudinal unpolarized current through a ballistic 2DEG with α-SO coupling will induce a nonequilibrium spin accumulation which has opposite signs for the two lateral edges. The discussion was extended with the investigation of the SHE in multiprobe ballistic SO coupled semiconductor bridges [14] i.e. a device where longitudinal leads are attached to ballistic quantum-coherent 2DEG in a semiconductor heterostructure [13,14]. The latter device can be assumed as a crossing junction between two Q1D wires [15]. In this kind of devices the effects of the β-SO coupling can be relevant as was discussed in reference [16] by giving a localization of the spin currents in a Q1D wire. It follows that the transverse profile of the out-of-plane $S_z(\mathbf{r})$ component of the spin accumulation develops two peaks of opposite signs in the lateral probes of the junction (2 and 4 in Fig. 1) when an unpolarized spin current is injected in the lead 1. Upon reversing the bias voltage (V_{13}), the edge peaks flip their sign $\langle S_z(\mathbf{r})\rangle_V = -\langle S_z(\mathbf{r})\rangle_{-V}$.

In this paper we discuss the spin polarization of the current in the presence of β-SO interaction in X-shaped [17] four-probe (Fig. 1 top) and T-shaped [18] three-probe (Fig. 1 bottom) nanometric cross junctions. We focus on single-channel transport and investigate with a numerical semiclassical approach the spin accumulation in the transverse leads. We will show why a β coupling scheme results in better performances and a different working principle as compared to equivalent structures exploiting the α coupling.

2 Model and theoretical approach

2.1 β-SO coupling and effective magnetic field

The β coupling term stems from equation (1) as

$$\hat{H}_{SO}^{\beta} = \frac{\lambda^2}{\hbar}\hat{\sigma_z}\left[\nabla V(x) \times \hat{\mathbf{p}}\right]_z. \tag{2}$$

This SO term can be seen as the interaction of the electron spin with the magnetic field appearing in the rest frame of the electron. In a Q1D wire, where a parabolic confinement along ξ ($\xi \equiv x$ for leads 1 and 3 and $\xi \equiv y$ for leads 2 and 4) with force ω_d is considered ($V(\mathbf{r}) \equiv V(\xi) = \frac{m^*\omega^2}{2}\xi^2$), it follows

$$\hat{H}_{SO}^{\beta} = \frac{\beta}{\hbar}\frac{\xi}{l_\omega}\left(\hat{\sigma} \times \hat{\mathbf{p}}\right)_\xi \simeq i\beta\frac{x}{l_\omega}\sigma_z\frac{\partial}{\partial\eta}. \tag{3}$$

Here $l_\omega = (\hbar/m^*\omega)^{1/2}$ is the typical spatial scale, η is the other direction in the 2DEG ($\eta \perp \xi$), and we assume $\langle p_z\rangle = 0$, because in a junction patterned in the plane of a 2DEG the motion perpendicular to the plane of the electron gas is quantum mechanically frozen out.

Thus, as we discussed in a previous paper [16], in a Q1D wire a uniform *effective magnetic field* B_{eff} is present along z ($B_{\mathit{eff}} = \lambda^2\, {m^*}^2\omega_d^2 c/\hbar$) directed up or down according to the sign of S_z.

The discussion reported above for a Q1D wire can be generalized to a device patterned in a 2DEG. The Hamiltonian of an electron moving in a 2D device defined by a generic confining potential $V_c(r)$ in which the α-SO term is negligible can be written as

$$\begin{aligned} H &= \frac{\mathbf{p^2}}{2m^*} + \frac{\lambda^2}{\hbar}e\left(\mathbf{E}(\mathbf{r}) \wedge \mathbf{p}\right)_z \sigma_z + V_c(\mathbf{r}) \\ &= \frac{\pi^2}{2} + V_c(\mathbf{r}) - \frac{\lambda^4 m^*}{2\hbar^2}e^2\left|\mathbf{E}(\mathbf{r})\right|^2, \end{aligned} \tag{4}$$

where $\pi_i = (p_i - \epsilon_{ijz}\frac{\lambda^2}{\hbar}m^* e E_j \sigma_z)$ and $\mathbf{E}(\mathbf{r}) = \nabla V_c(\mathbf{r})$.

The commutation relation

$$[\pi_x, \pi_y] = -i\hbar\left(\frac{\lambda^2}{\hbar}m^* e \nabla\cdot\mathbf{E}\right)\sigma_z \equiv -i\hbar\frac{e}{c}B_{\mathit{eff}}(\mathbf{r})\sigma_z$$

is equivalent to that of a charged particle in a transverse magnetic field, but here the sign of $B_{\mathit{eff}}(\mathbf{r})$ depends on the direction of the spin along $\hat{z}$.

2.2 Models for the junctions

In a four-probe cross junction sample (Fig. 1 bottom), the confining electrostatic potential V_X for an electron is

not exactly known. However, it is plausible that there has to be a potential minimum at the center of the junction. In this respect, it would be appropriate to qualitatively model the smooth potential walls as

$$V_X(x,y) = \frac{m^*}{2}\omega_d^2 R^2 \frac{x^2 y^2}{(R^2+x^2)(R^2+y^2)}, \qquad (5)$$

where l_ω can be related to the effective width of the wires, W and R to the effective radius of the crossing zone. Analogously, for a T shaped cross junction, we write

$$V_T(x,y) = \frac{m^*\omega_d^2 R^2}{2}\frac{y^2}{R^2+y^2}\left(\frac{x^2}{R^2+x^2}\vartheta(-y)+\vartheta(y)\right), \qquad (6)$$

where $\vartheta(y) \sim (1+\tanh(y/\rho))/2$. In both cases, it follows the asymptotic behaviour corresponding to parabolic QWs, while $B_{eff}(x,y)$ is a not homogeneous field with a constant asymptotic value, $\widetilde{B}_{eff} = B_{eff}(x,-\infty)$. Next, our results will be given as a function of the ratio ω_c/ω_d with $\omega_c = e\widetilde{B}_{eff}/(m^*c)$.

2.3 Ballistic transport and theoretical approach

When the characteristic sizes of semiconductor devices are smaller than the elastic mean free path of charge carriers, the carrier transport becomes ballistic. It follows that the transport can be studied starting from the probability of transmission from one probe to another one following the Büttiker-Landauer formalism [19].

The calculation of the transmissions amplitude is based on the simulation of classical trajectories of a large number of electrons with different initial conditions. We want to determine the probability $T_{1j}^{s,s'}$ of an electron with spin s to be transmitted to lead j with spin s' when it is injected in lead 1. These coefficient can be determined from the classical dynamics of electrons injected at $y_0 = -7.5\, l_\omega$ (emitter position) with an injection probability following a spatial distribution $p_0(x_0,y_0) \propto e^{-x_0^2/l_\omega^2}$ as in reference [20]. The total energy ε of a single electron is composed by the free electron energy ε_y^0 for motion along y and the energy of the transverse mode considered ε_x^0 due to the parabolic confinement ($\varepsilon_x = \hbar\omega_d/2$ for the lowest channel).

Thus, we have calculated $T_{ij}^{s,s'}$ determined by numerical simulations of the classical trajectories injected into the junction potential V_c with boundary conditions [17] $\mathbf{r}(0) \equiv (x_0,y_0); \mathbf{v}(0) \equiv \mathbf{v}_0$, each one with a weight $p_0(x_0)$. In general these transmission amplitudes can depend on the position of the collectors along the probes.

Before passing to the discussion about our results, we want to point out that a comparison with theoretical and experimental results allowed us to test our approach. In fact, in reference [17] we investigated the effects on the X-junction transport due to a quite small external magnetic field, B_{ext}, by focusing on the so called *quenched region*. The measured "quenching of the Hall effect" [21] is a suppression of the Hall resistance or "a negative Hall resistance" R_H for small values of B_{ext}. The results reported in reference [17] showed a good agreement with the experimental data by confirming the reliability of our approach.

3 Results

The Lorentz force due to the effective field B_{eff} deflects spin-↑ and spin-↓ electrons in opposite transverse directions by giving a spin accumulation $\langle S_z(x)\rangle$ in the transverse probes (2 and 4) depending on the transverse coordinate x.

In Figure 2 we show the profile of $\langle S_z(x)\rangle$ in the X-junction obtained by moving the collectors along the x direction. $\langle S_z(x)\rangle$ corresponds to the spin polarization

$$\langle S_z\rangle = \frac{T_{i1}^{\uparrow\uparrow} - T_{i1}^{\downarrow\downarrow}}{T_{i1}^{\uparrow\uparrow} + T_{i1}^{\downarrow\downarrow}},$$

in this special case where $T_{ij}^{\uparrow\downarrow} = T_{ij}^{\downarrow\uparrow} = 0$, because of the commutation between $\hat{S}_z$ and $\hat{H}_{SO}^{\beta}$. We observe a plateau in the top panel for values of ω_c/ω_d larger than 10^{-2} at a large distance from the crossing zone. We can also observe the presence of *quenching*, i.e. a negative $\langle S_z(x)\rangle$ for a smaller value of ω_c/ω_d, in agreement with the results reported in reference [17].

In Figure 3 we report the results corresponding to a T-junction. Also in this case, a plateau is present for strong effective fields, whereas a quenching behaviour can characterize the small effective field regime.

The correspondence between this spin accumulation and the presence of a transverse SH current was discussed in reference [13]. The current I_i in the lead i of a four-probe junction with chemical potentials $\mu_j = eV_j$ attached to leads j can be expressed in terms of the T_{ij} by $I_i = e^2/h\sum_j T_{ij}(V_i - V_j)$, and normalization requires $\sum_j T_{ij} = 1$ [19,20]. Here $I_1 = I_1^{\uparrow} + I_1^{\downarrow}$ is the injected current, I_{i1}^s is the charge current outgoing from the lead i corresponding to the spin polarization s. Thus, there should be two spin polarized (charge) currents, I_H^s in the x direction, from right to left, given by $I_H^s = I_{41}^s - I_{21}^s$. When we take into account a spin unpolarized injected current, I_1, it follows from the spin dependence of the effective magnetic field that $I_{11}^{\uparrow} = I_{11}^{\downarrow}$,$I_{31}^{\uparrow} = I_{31}^{\downarrow}$, $I_{21}^{\uparrow} = -I_{21}^{\downarrow}$ and $I_{41}^{\uparrow} = -I_{41}^{\downarrow}$. The symmetry of the device implies that the charge Hall current vanishes, $I_H = I_H^{\uparrow} + I_H^{\downarrow} = 0$. In this case we can define also the Spin Hall current as

$$I_{sH} = \frac{\hbar}{2e}\left(I_H^{\uparrow} - I_H^{\downarrow}\right). \qquad (7)$$

Thus, in our cases, it follows that to an injected current I_0 in the lead 1 it corresponds a transverse SH current given by equation (7), i.e. the spin accumulation will push the pure spin current I_{sH} into the transverse probes. This current and its polarization can be inferred from the profiles of $\langle S_z(x)\rangle$ in Figures 2 and 3.

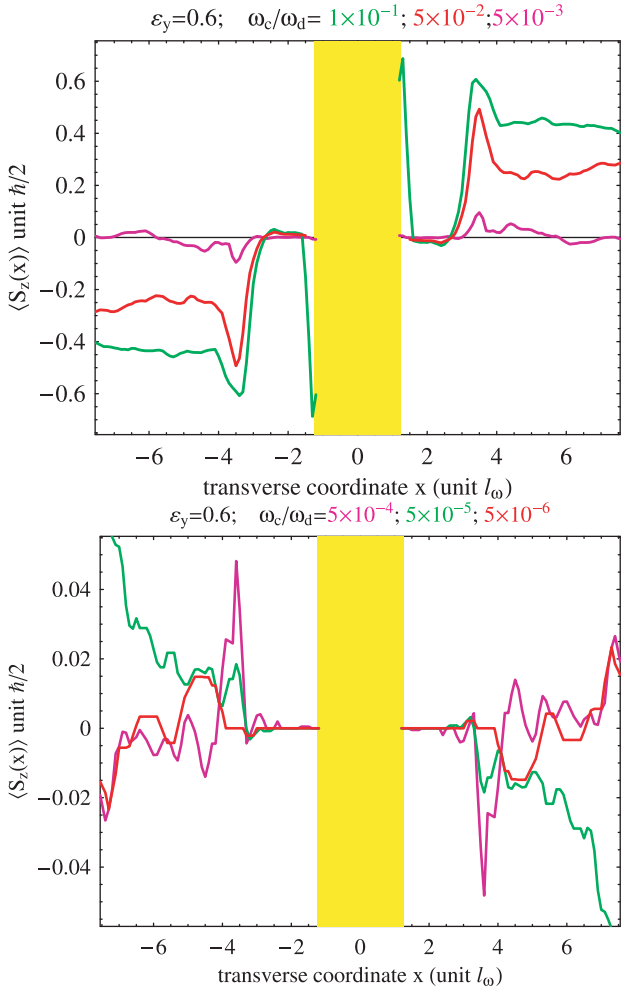

Fig. 2. (Color online) The one-dimensional transverse spatial profile of the spin accumulation $\langle S_z(x)\rangle$ across the transverse probes (2 and 4) of the ballistic X-junction with vanishing α-coupling, while the β-SO coupling corresponds to ω_c/ω_d ranging from 10^{-6} to 10^{-1}. We observe a kind of plateau in the top panel $\omega_c/\omega_d \gtrsim 10^{-2}$ at a large distance from the crossing zone. We observe the presence of *quenching*, i.e. a negative $\langle S_z(x)\rangle$ corresponding to a negative SH resistence [17], in the bottom panel $\omega_c/\omega_d \lesssim 10^{-4}$ at a large distance from the crossing zone. The electrons are injected at $y \sim -7.5 l_\omega$ where we suppose it is located the emitter, while the collectors are moved along the x direction.

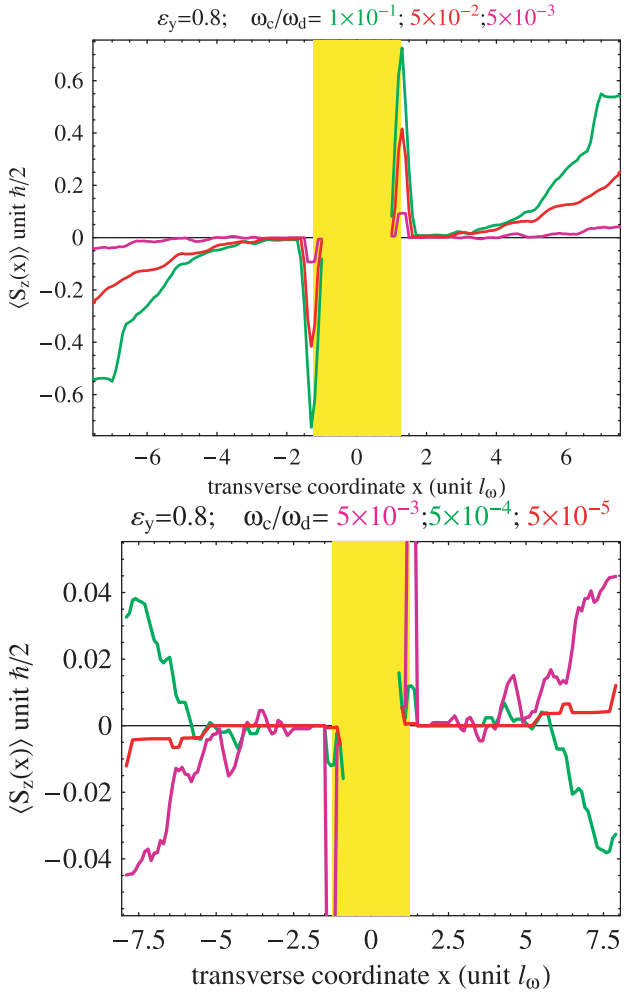

Fig. 3. (Color online) The one-dimensional transverse spatial profile of the spin accumulation $\langle S_z(x)\rangle$ across the transverse probes (2 and 4) of the ballistic T-junction with vanishing α-coupling while the β-SO coupling corresponds to ω_c/ω_d ranging from 10^{-5} to 10^{-1}. We observe the increasing of $\langle S_z(x)\rangle$ as the distance from the crossing zone increases. We observe the presence of *quenching*, i.e. a negative $\langle S_z(x)\rangle$ corresponding to a negative SH resistence [17], in the bottom panel $\omega_c/\omega_d \sim 5 \times 10^{-4}$. The electrons are injected at $y \sim -7.5 l_\omega$.

However, according the discussion of reference [13], in many cases the detection of the currents requires one to measure the spin accumulation that they deposit at the sample edges [22].

4 Discussion

The theoretical technique employed in the paper deserves a detailed discussion.

We can compare the results presented here for the X junction with the ones reported in reference [23]. In that paper a more standard quantum approach to calculating the transmission amplitudes was used, and the agreement between the approaches can be found both qualitatively and quantitatively just for the strongest values of the effective magnetic field (the plateaus in the top panel of Fig. 2 found for $\omega_c/\omega_d > 10^{-2}$).

When the effective magnetic field decreases, in the *quenching* regime, the results obtained by using the different approaches can begin to differ from each other. The semiclassical approach, proposed here, can be in these cases more suitable. This was shown by investigations about the effects of a transverse external magnetic field on transport through micrometric ballistic junctions, carried out about 20 years ago. In fact several magneto-transport

anomalies were found in these devices, among these the quenched or negative Hall resistance, bend resistances and a feature known as the last Hall plateau. The physical origin of these anomalies may be understood in the Büttiker-Landauer scattering approach and it was shown that many observed effects, e.g. the classical Hall plateau, have a classical origin and can be reproduced, based on classical trajectories. Other anomalies were explained on the ground of a strong geometry dependence; in fact, in the presence of a transverse magnetic field, the resistances measured in narrow-channel geometries are mainly determined by the scattering processes at the junctions with the side probes which depend strongly on the junction shape [24]. Thus the rounded corners (present in a realistic situation) at the junction between the main channel and the side branches lead to the suppression (*quenching*) of the Hall resistance at low magnetic fields, while a Hall bar with straight corners does not show a generic suppression of the Hall resistance [25].

The analysis of the quenching regime in a nanojunction allowed us to test the theoretical approach presented in this paper; in fact the discussed semiclassical method is the most suitable to reproduce the effects due to the real shape of the junction at low magnetic field as can be argued by a comparison between the experimental results (Fig. 1 top of Ref. [21]) and the theoretical prediction shown in Figure 2 top of reference [17]. Thus we suspect that the semiclassical approach is the most suitable to investigate the spin transport through nanometric ballistic junctions when the effective magnetic field is rather small.

The strength of the SO-couplings terms deserves an accurate discussion. Both terms depend on the nature of the heterostructure and can be differ even by orders of magnitude when using different materials. Moreover the α term arising from the quantum-well electric field directed along the z-axis is considerably diminished in square quantum wells [26], while the β term strongly depends on the effective width of the Q1D devices forming the junctions.

The typical value of $\alpha \equiv \lambda^2 E_z e$ in 2DEGs ranges from 10^{-13} to 10^{-10} eV m. The effective value of λ in the 2DEG at interface InGaAs/InP can be obtained from the measured value of α (5×10^{-12} eV m as in Ref. [27]) and from the calculated band diagram of the same structures. This is in agreement with the values used in reference [5], where $\alpha \sim 10^{-11}$–10^{-12} eV m, $\beta \sim 0.1\alpha$ (W of some hundreds of nms) and λ^2 ∼0.2–2 nm^2. This estimate does not consider the contribution to α deriving from the different values of the wave function at the two interfaces of the quantum well For GaAs heterostructures λ^2 is one order of magnitude less than in InGaAs/InP, while for HgTe based heterostructures λ^2 can be larger by one order of magnitude or more, up to some tens of nm^2, as discussed in reference [28]. These values are of the same order of magnitude as the ones used in reference [13], where α ranges from 4×10^{-11} to 2×10^{-10} eV m. For our results the fundamental parameter is given by the ratio ω_c/ω_d. Because the lithographical width of a wire defined in a 2DEG can range from some hundreds to a few tens of nm (20 nm as in Ref. [29]), we can assume that the ratio ω_c/ω_d runs from 10^{-6} to 10^{-1}. In any case W should be larger than λ_F, so that at least one mode is occupied.

The value of the spin accumulation predicted for the β-SO coupling in the T and X junctions is some orders of magnitude larger than the one predicted in reference [13] and is due to a quite strong α-SO interaction . We can suppose that the typical values of α used there corresponds to the larger values of ω_c/ω_d used in our letter. There it was found $\langle S_z(x) \rangle \lesssim 10^{-3}$, i.e. a value 2 order of magnitudes smaller than the values found by us. Thus we conclude that in narrow ballistic junctions the β-SO coupling can be quite relevant and is the main responsible of the spin accumulation.

We acknowledge the support of the grant 2006 PRIN "Sistemi Quantistici Macroscopici-Aspetti Fondamentali ed Applicazioni di strutture Josephson Non Convenzionali".

References

1. D.D. Awschalom, D. Loss, N. Samarth, *Semiconductor Spintronics and Quantum Computation* (Springer, Berlin, 2002); B.E. Kane, Nature **393**, 133 (1998)
2. S.A. Wolf, D.D. Awschalom, R.A. Buhrman, J.M. Daughton, S. von Molnar, M.L. Roukes, A.Y. Chtchelkanova, D.M. Treger, Science **294**, 1488 (2001)
3. *The Hall Effect and its Applications*, edited by C.L. Chien, C.W. Westgate (Plenum, New York, 1980)
4. L.D. Landau, E.M. Lifshitz, *Quantum Mechanics* (Pergamon Press, Oxford, 1991)
5. A.V. Moroz, C.H.W. Barnes, Phys. Rev. B **61**, R2464 (2000)
6. G. Dresselhaus, Phys. Rev. **100**, 580 (1955)
7. M.J. Kelly, *Low-dimensional semiconductors: material, physics, technology, devices* (Oxford University Press, Oxford, 1995)
8. T.J. Thornton, M. Pepper, H. Ahmed, D. Andrews, G.J. Davies, Phys. Rev. Lett. **56**, 1198 (1986)
9. M.I. D'yakonov, V.I. Perel', JETP Lett. **13**, 467 (1971)
10. S. Murakami, N. Nagaosa, S.C. Zhang, Science **301**, 1348 (2003)
11. J. Sinova, D. Culcer, Q. Niu, N.A. Sinitsyn, T. Jungwirth, A.H. MacDonald, Phys. Rev. Lett. **92**, 126603 (2004)
12. M.L. Sheng, D.N. Sheng, C.S. Ting, Phys. Rev. Lett. **94**, 016602 (2005); E.M. Hankiewicz, L.W. Molenkamp, T. Jungwirth, J. Sinova, Phys. Rev. B **70**, 241301(R) (2004)
13. B.K. Nikolic, S. Souma, L.P. Zarbo, J. Sinova, Phys. Rev. Lett. **95**, 046601 (2005)
14. B.K. Nikolic, L.P. Zarbo, S. Souma, Phys. Rev. B **72**, 075361 (2005)
15. The width W of each Q1D corresponding to the device proposed in reference [13] ranges from ∼25 nm up to 100 nm
16. S. Bellucci, P. Onorato, Phys. Rev. B **73**, 045329 (2006)
17. S. Bellucci, P. Onorato, Phys. Rev. B **74**, 245314 (2006)
18. A.A. Kiselev, K.W. Kim, Appl. Phys. Lett. **78**, 775 (2001)
19. M. Büttiker, Phys. Rev. Lett. **57**, 1761 (1986)
20. T. Geisel, R. Ketzmerick, O. Schedletzky, Phys. Rev. Lett. **69**, 1680 (1992)

21. C.J.B. Ford, S. Washburn, M. Büttiker, C.M. Knoedler, J.M. Hong, Phys. Rev. Lett. **62**, 2724 (1989)
22. Y.K. Kato, R.C. Myers, A.C. Gossard, D.D. Awschalom, Science **306**, 1910 (2004); J. Wunderlich, B. Kaestner, J. Sinova, T. Jungwirth, Phys. Rev. Lett. **94**, 047204 (2005)
23. S. Bellucci, P. Onorato Phys. Rev. B **75**, 2335326 (2007)
24. G. Timp, H.U. Baranger, P. deVegvar, J.E. Cunningham, R.E. Howard, R. Behringer, P.M. Mankiewich, Phys. Rev. Lett. **60**, 2081 (1988)
25. H.U. Baranger, A.D. Stone, Phys. Rev. Lett. **63**, 414 (1989)
26. T. Hassenkam, S. Pedersen, K. Baklanov, A. Kristensen, C.B. Sorensen, P.E. Lindelof, F.G. Pikus, G.E. Pikus, Phys. Rev. **55**, 9298 (1997)
27. G. Engels, J. Lange, Th. Schäpers, H. Lüth, Phys. Rev. B **55**, R1958 (1997)
28. X.C. Zhang, A. Pfeuffer-Jeschke, K. Ortner, V. Hock, H. Buhmann, C.R. Becker, G. Landwehr, Phys. Rev. B **63**, 245305 (2001)
29. M. Knop, M. Richter, R. Maßmann, U. Wieser, U. Kunze, D. Reuter, C. Riedesel, A.D. Wieck Semicond. Sci. Technol. **20**, 814 (2005)